WAVE–BARRIER INTERACTION IN A VISCOPLASTIC MEDIUM

G. M. Lyakhov and K. S. Sultanov

UDC 624.131+539.215

In [1, 2], a viscoplastic soil model was proposed. Below, on the basis of this model, the problem of the interaction of a plane one-dimensional wave and a fixed or displaceable barrier is solved using a computer and the method of characteristics. In [2, 3] the wave-propagation problem was solved on the basis of the same model. The results of blast-wave-parameter measurements, indicating that the viscous and plastic properties of soils have an important effect on the wave-propagation characteristics, were presented in [2, 4-6].

In accordance with the model proposed in [1], in dense media two limiting nonlinear volume compression diagrams, $\sigma_D(\varepsilon)$ and $\sigma_S(\varepsilon)$, should be taken into account. These correspond to dynamic loading ($\dot{\varepsilon} \to \infty$) and to the equilibrium state of the medium ($\dot{\varepsilon} \to 0$) (static loading). Unloading is not governed by the same equations as loading, which leads to the formation of residual strains. The total strain of an element is $\varepsilon = \varepsilon_1 + \varepsilon_2$, where ε_1 is associated with the instantaneous compression and ε_2 with the compression developing over a finite time.

At small loads the limit relations are assumed to be linear and the behavior of the medium [1, 2] is determined by the following sequence of equations:

for impact loading (at the discontinuity),

$$\sigma = E_D\varepsilon; \tag{1}$$

for a continuous increase of stress (stress loading),

$$\dot{\varepsilon} + \mu\varepsilon = \dot{\sigma}/E_D + \mu\sigma/E_S; \tag{2}$$

for decreasing stress but increasing ε_2 (stress unloading),

$$\dot{\varepsilon} + \mu\varepsilon = \dot{\sigma}/E_R + \mu\sigma(1/E_S - 1/E_D + 1/E_R) + \mu\sigma_m(1/E_D - 1/E_R); \tag{3}$$

for decreasing stress and $\varepsilon_2 = \text{const}$ (ε_2 assumed irreversible),

$$\dot{\sigma} = E_R\dot{\varepsilon}, \tag{4}$$

where $\mu = E_DE_S/(E_D - E_S)\eta$ (viscosity parameter); E_D is the dynamic and E_S the static compressive modulus; E_R is the unloading modulus; η is the coefficient of viscosity; and σ_m is the maximum particle stress.

The wave in the medium is created by the load in the initial cross section $r = 0$, which varies according to the law

$$\sigma = \sigma_{\max}(1 - t/\theta),\ 0 \leqslant t \leqslant \theta;\ \sigma = 0,\ t \geqslant \theta. \tag{5}$$

At a distance r^* there is a barrier of incompressible material of mass m per unit area bounded by two parallel planes. The medium beyond the barrier is the same as that in front of it. It is proposed to determine the parameters of the incident, reflected, and transmitted waves, the load on the barrier, and the motion of the barrier.

For a particle in the state defined by (3), in the presence of the secondary increase in stress caused by the arrival of the reflected wave, the equation remains valid until σ_m is reached (maximum stress in incident wave), after which Eq. (2) is satisfied. For a particle in the state defined by (4), the equation remains valid up to the value of σ corresponding to the beginning of unloading with respect to ε_2, after which Eq. (3) is satisfied and, beyond σ_m, Eq. (2).

We will use the Lagrangian variables h = mass and t = time. The solution reduces to the integration of the system of basic equations of motion

$$\frac{\partial u}{\partial t} - \frac{\partial \sigma}{\partial h} = 0,\quad \frac{\partial u}{\partial h} - \frac{1}{\rho_0}\frac{\partial \varepsilon}{\partial t} = 0,\quad h = \rho_0 r,$$

Moscow. Translated from Zhurnal Prikladnoi Mekhaniki i Tekhnicheskoi Fiziki, No. 4, pp. 108-116, July-August, 1978. Original article submitted June 30, 1977.

0021-8944/78/1904-0509$07.50

which is closed successively by the equations (1)-(4); ρ_0 is the initial density of the medium.

The boundary conditions are as follows: In the initial section Eq. (5) is given; at the incident and transmitted wave fronts

$$\sigma = -Au,\ h = At,\ A = \sqrt{E_D\rho_0} = c_0\rho_0,$$

c_0 is the speed of sound determined from the dynamic diagram; at the barrier

$$mdu/dt = \sigma_1 - \sigma_2,\ h = h^* = \rho_0 r^*,$$

where σ_1 is the barrier load associated with the incident wave and σ_2 is that associated with the transmitted wave (when $m = \infty$ we obtain $u = 0$); at the reflected wave front

$$\sigma_3 - \sigma_1 = A(u_3 - u_1),\ h = -At + 2h^*,$$

where σ_1, u_1, and σ_3, u_3 are the stresses and particle velocities in the incident and reflected waves, respectively.

We now go over to dimensionless Lagrangian variables and dimensionless stresses, strains, particle velocity, and barrier mass;

$$x = \mu r/c_0 = \mu h/A,\ \tau = \mu t,\ \sigma^0 = \sigma/\sigma_{max},$$

$$u^0 = -Au/\sigma_{max},\ \varepsilon^0 = E_D\,\varepsilon/\sigma_{max},\ m^0 = \mu m/A.$$

We denote $E_D/E_S = \gamma$, $E_D/E_R = \beta$, and $x^* = \mu h^*/A = \mu r^*/c_0$. In the new variables the problem parameters are γ, β, $\mu\theta$, m^0, and x^*.

The solution was obtained on a BÉSM-6 computer for the nine variants of Table 1, using the method of characteristics with $x^* = 6$.

In all cases, apart from variant 9, the load in the initial section corresponded to Eq. (5) and $\beta = 0.5$; for variant 9 we took $\sigma = \sigma_{max}(1 - t/\theta)^3$, and $\beta = 0.4$.

Experimental values of the characteristics of certain soils [2], required for the transition to dimensional quantities, are presented in Table 2, where w is the moisture content of the soil.

We will examine the general laws of wave–barrier interaction with reference to the example of variant 6. In Fig. 1a-c we have plotted the $\sigma^0(\tau)$, $\varepsilon^0(\tau)$, and $u^0(\tau)$ curves in various cross sections of the medium for passage of the incident, reflected, and transmitted waves. Without loss of generality, it may be assumed that the barrier is infinitely thin but has finite mass m^0. The appearance of the wave beyond the barrier corresponds to the moment of arrival of the precursor of the incident wave. Curves 0-3 relate to the distances $x^* = 0$, 1.5, 3, and 4.5 (in front of the barrier), curves 4 and 5 to the distance $x^* = 6$ (at the barrier, front and rear), and curves 6-9 to the distance $x^* = 7.5$, 9, 10.5, and 15 (beyond the barrier).

The incident wave is led by a precursor with a discontinuity of all the parameters at the front (discontinuities are denoted by circles). Beyond the discontinuity the parameters increase and decrease continuously. With increase in the distance from the initial cross section the wave gradually broadens, the discontinuity tends to zero, and the time taken by the parameters to reach the maximum increases. The development of the strain and particle velocity lags behind the stress.

As the discontinuity approaches the barrier, the stress doubles, as in a linear-elastic medium, since at the discontinuity the viscous properties are suppressed. The reflected wave travels from the barrier to the initial section; at the same time, the load on the barrier increases, and the barrier is set in motion, which creates a continuous transmitted compression wave beyond the barrier. The broadening process is continued in the reflected wave, the discontinuity at the wave front being quickly assimilated. In the particles there is a secondary increase in stress and strain, which then decrease again. As it approaches the initial section, the reflected wave is attenuated, and the secondary maxima decrease.

In the initial section, on the arrival of the reflected wave, the wave-creating load still has a large value. The wave traveling from the barrier is reflected from this section, which gives rise to a third wave moving toward the barrier and producing a further increase in stress and strain. Interaction of the third wave and the barrier generates a fourth wave

TABLE 1

Variant	1	2	3	4	5	6	7	8	9
$\mu\theta$	5	10	50	5	10	50	5	20	10
m^0	∞	∞	∞	10	10	10	10	20	10
γ	2	2	2	2	2	2	1,1	2	4

TABLE 2

Soil	$\rho_0 \cdot 10^{-3}$, kg/m^3	w, %	$E_D \cdot 10^{-5}$, H/m^3	γ	μ, sec^{-1}	η, N·sec/m^2
Sand	1,6	7,5	160	2	500	$3{,}2 \cdot 10^4$
Loam	1,8	12	500	2,5	220	$1{,}5 \cdot 10^5$
Clay	1,8	20	450	4,5	1000	$1{,}3 \cdot 10^4$

traveling toward the initial section. The second maximum of the barrier load on the incident-wave side is lower than the first. The interaction of the third wave and the barrier leads to an increase in barrier velocity and to the appearance of a secondary compression wave beyond the barrier, which causes a new increase in the parameters. The maximum values of σ^0, ε^0, and u^0 are higher in this wave than in the first — in this way the progressive transfer of energy from the region in front of the barrier to the region beyond it is accomplished.

At small $\mu\theta$ there is no secondary increase in barrier load and no secondary wave beyond the barrier, since the wave reflected from the barrier exhausts itself on the way to the initial section.

Figure 2 shows the wave propagation at different values of the load and barrier parameters. Curve 0 corresponds to the incident and transmitted wave fronts, curves 1°-6° to the front of the wave reflected from the barrier, and curves 1*-6*, 1-6, and 4**-6** to the stress maxima of the incident, reflected, and transmitted waves, respectively. The velocities of the incident- and transmitted-wave fronts do not depend on the load parameters and the barrier mass, but only on the properties of the medium. The velocity of the incident-wave maximum decreases with increase in $\mu\theta$ but increases with distance from the initial section. On the first-loading intervals the velocity of the reflected-wave front is equal to the incident wave velocity, but on the stress-unloading intervals it has a greater value determined by the unloading modulus. The barrier load reaches a maximum at the moment of arrival of the incident-wave maximum. The velocity of the reflected-wave maximum increases with distance from the barrier. It is substantially greater than the velocity of the incident-wave maximum. As $\mu\theta$ increases, so does the time required to reach the maximum of the load on the front of the barrier. The maximum of the wave reflected from a fixed barrier moves faster than that of the wave reflected from a displaceable barrier.

Figure 2 also shows the variation of the load $\sigma^0(\tau)$ in the initial section at the three values $\mu\theta$ = 5, 10, and 50, corresponding to cases 1 and 4, 2, and 5, and 3 and 6.

In Fig. 3, we have plotted the barrier load for viscoplastic, elastic, and plastic models. Curves 1-6 give the load on the front and curves 4°-6° the load on the rear face of a barrier in a viscoplastic medium. As before, the numbering of the curves corresponds to the order of the variants. Curves 1*-3* relate to the load on a fixed barrier calculated in accordance with the model of a linear-elastic medium for $\mu\theta$ = 5, 10, and 50, respectively. The modulus of elasticity was taken equal to the dynamic compression modulus for the viscous medium. Curves 2** and 3** give the fixed-barrier load calculated on the basis of the model of a plastic medium with compressive modulus equal to the dynamic modulus of the viscous medium and with unloading at constant strain ($\mu\theta$ = 10 and 50, respectively). In accordance with [7], as far as the sudden drop the barrier load is determined by the following equations:

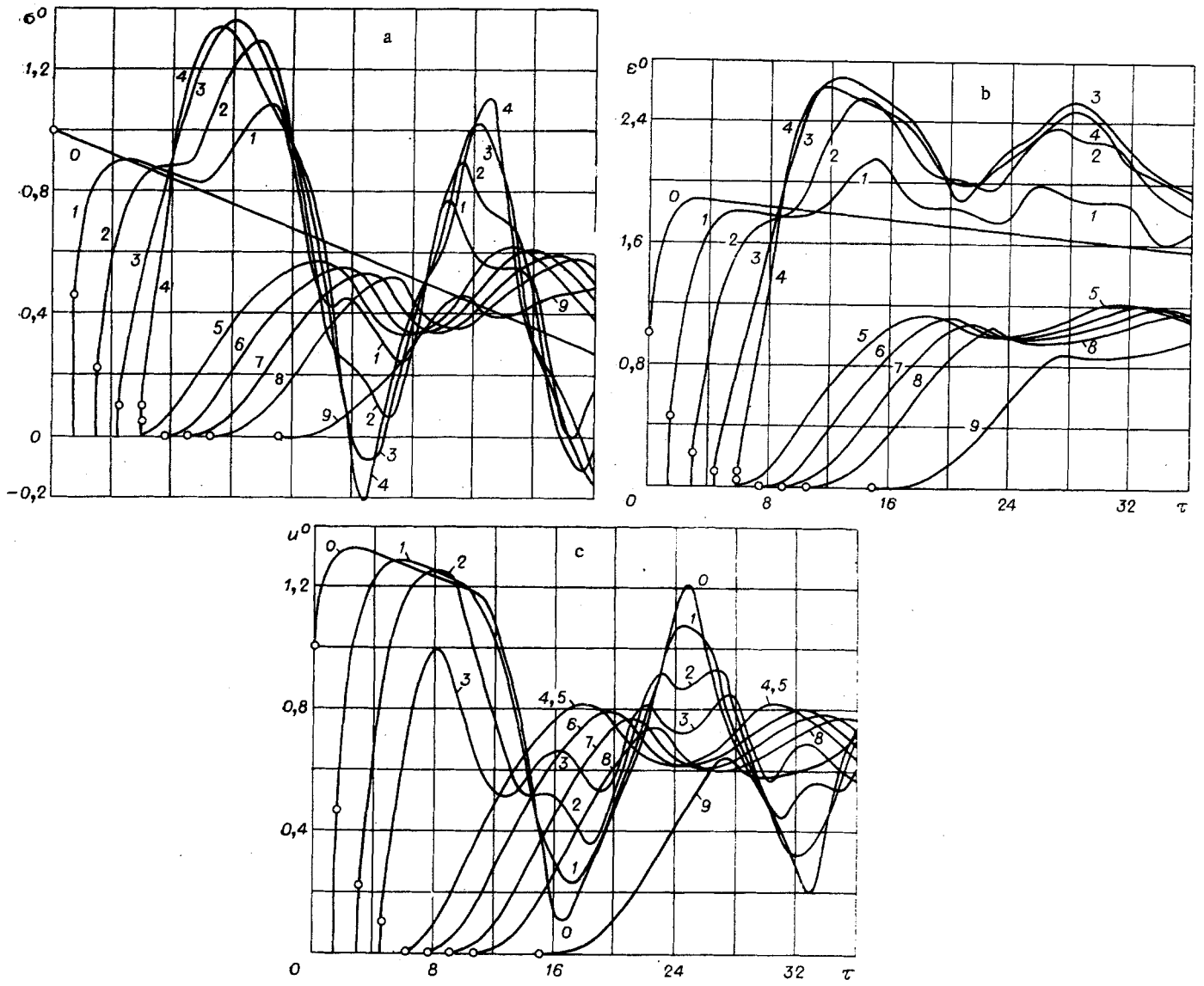

Fig. 1

in a plastic medium,

$$p^0 = 2[1 + \tau/\mu\theta - 3\tau^*/2\mu\theta + \tau^* \ln (2 - \tau/\tau^*)/\mu\theta];$$

in a linear-elastic medium,

$$p^0 = 2[1 + (\tau^* - \tau)/\mu\theta].$$

In a plastic medium the load falls to a value corresponding to the initial section.

From a comparison of curves 1-3 and 4-6 it follows that displaceability of the barrier leads to a decrease in the load on the front face.

In the case of variant 7, in the wave approaching the barrier the maximum stress is reached abruptly at the front (the wave is not smeared out); consequently, the load on the leading face has a maximum at the moment of arrival of the front. From a comparison of curves 7 and 4 it follows that a decrease in γ, equivalent to convergence of the static and dynamic compression diagrams, leads to an increase in the maximum value of the load, changes its character (to impact), but reduces its duration. As $\gamma \to 1$, the viscous medium goes over into an elastic Hookean medium. At $\gamma = 1.1$, the wave still decays appreciably on the way to the barrier, but, as in the case of a Hookean medium, there is no longer any broadening. The value $\gamma = 1.0$-1.5 relates to rocks. In soils γ has greater values, in the range 2-4.5 [2].

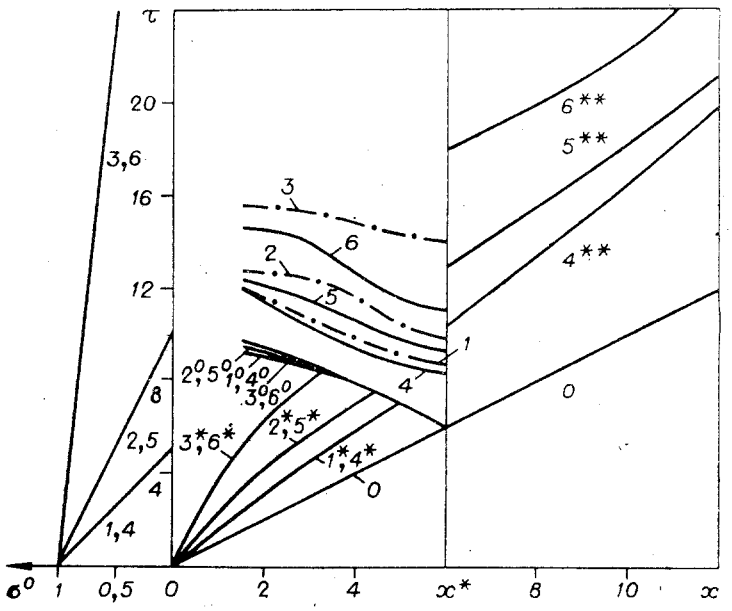

Fig. 2

An increase in $\mu\theta$ (θ increases while μ remains constant) leads to an increase in the maximum value of the load and to an increase in its duration of action.

The dynamic compression diagram of the plastic medium is assumed to be linear; therefore, the wave does not broaden but remains an impact wave. In this case the load on the barrier increases abruptly.

The dimensionless acceleration of the barrier

$$du^0/d\tau = (\sigma_1^0 - \sigma_2^0)\, m^0,$$

where σ_1^0 and σ_2^0 are the loads on the front and rear faces, respectively.

In the elastic and plastic media considered the maximum of σ_1^0 is reached as the impact-wave front approaches the barrier. Its value does not depend on the barrier mass. At this point of time, $\sigma_2^0 = 0$ for all values of m^0. In the course of time σ_1^0 decreases, while σ_2^0 increases to a maximum and then likewise decreases. Hence, it follows that the acceleration has a maximum at the approach of the wave front. For $m^0 = 10$ and $\mu\theta = 50$, in accordance with curves 3* and 2* in Fig. 3, the maximum accelerations are 0.2 and 0.188 in the elastic and plastic media, respectively.

In the medium with viscosity at $\gamma = 2$ and 4, the wave approaching the barrier also has a discontinuity at the wave front, but this is followed by a further increase in stress. The load on the front face increases for some time. At the same time, the load on the rear face also increases. The barrier acceleration reaches a maximum at the maximum value of the difference $\sigma_1^0 - \sigma_2^0$. When $m^0 = 10$ and $\mu\theta = 50$ (see curves 6 and 6° in Fig. 3) the maximum acceleration $du^0/d\tau = 0.105$ occurs at $\tau = 11.1$. The barrier acceleration is less in the viscous medium than in the elastic and plastic media.

Taking into account the second (dilatational) viscosity of the medium leads to broadening of the incident, reflected, and transmitted waves, as well as to a broadening of the barrier load and a reduction in its maximum value and in the maximum acceleration.

In Fig. 4 we have plotted the $\sigma^0(\varepsilon^0)$ curves for the passage of the incident and reflected waves through various cross sections and at the barrier; curves 1-3 relate to the viscous medium (variant 2) and to distances $x^* = 0.96$, 1.92, and 6 (at the barrier), respectively; curves 1*-3* relate to the plastic medium and to the same distances. In both cases the barrier is fixed, $\mu\theta = 10$. After the discontinuity at the precursor, with further continuous increase in stress the state of the viscous medium gradually moves away from the dynamic diagram toward the static diagram and crosses it into the region of higher strains. The arrival of the reflected wave causes a secondary increase in stress and strain. In the plastic medium the discontinuity is followed by unloading of the medium at constant strain and secondary

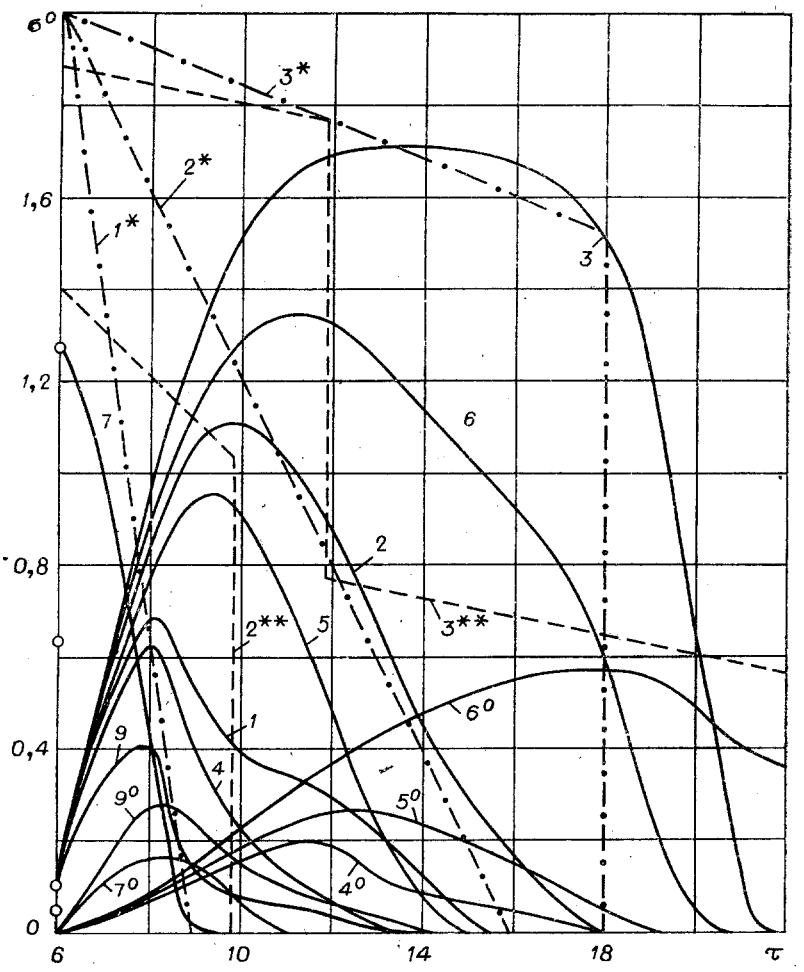

Fig. 3

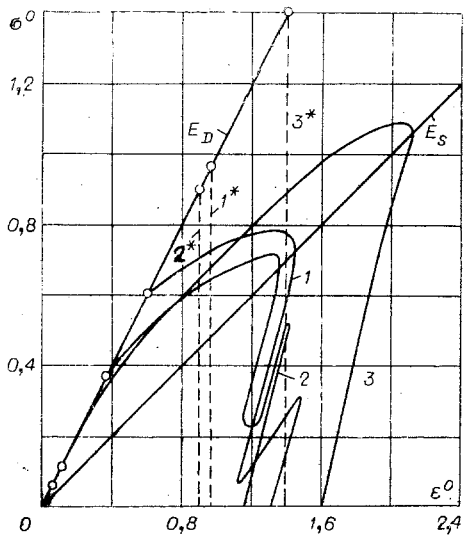

Fig. 4

unloading along the unloading line. In Fig. 4, lines E_D and E_S represent the dynamic and static compression diagrams for the viscous medium.

From the results of the calculations it follows that in the case of wave–barrier interaction tensile stresses may develop (see Fig. 1a), with the result that the medium loses its continuity. However, the maximum barrier loads and the maximum barrier accelerations are reached before the tensile stresses develop. Calculations at $\tau \geq 20$ were made to illustrate

the change in the parameters when the soil withstands tensile stresses $\sigma^\circ = -0.2$. Loss of continuity was not taken into account in formulating the problem.

The solution obtained shows that the laws of wave–barrier interaction depend importantly on both the plastic and the viscous properties of the medium. Viscosity leads to broadening of the reflected and transmitted waves and the barrier load and modifies their profile, at the same time reducing the maxima of the barrier load and acceleration.

LITERATURE CITED

1. G. M. Lyakhov, "Determination of the viscous properties of soils," Zh. Prkl. Mekh. Tekh. Fiz., No. 4 (1968).
2. G. M. Lyakhov, Fundamentals of Blast-Wave Dynamics in Soils and Rocks [in Russian], Nedra, Moscow (1974).
3. G. M. Lyakhov and Ya. A. Pachepskii, "Allowance for viscous and plastic properties in solving wave problems," Zh. Prikl. Mekh. Tekh. Fiz., No. 2 (1973).
4. Yu. I. Vasil'ev, L. A. Ivanova, and M. N. Shcherbo, "Measurement of the stresses and strains produced by blast waves in soils," Izv. Akad. Nauk SSSR, Fiz. Zemli, No. 1 (1969).
5. A. A. Vovk, Fundamentals of the Applied Geodynamics of Explosions [in Russian], Naukova Dumka, Kiev (1976).
6. S. S. Grigoryan, G. M. Lyakhov, and P. A. Parshukov, "Spherical blast waves in soils from stress and strain measurements," Zh. Prikl. Mekh. Tekh. Fiz., No. 1 (1977).
7. G. M. Lyakhov and N. I. Polyakova, Waves in Dense Media and Loads on Structures [in Russian], Nedra, Moscow (1967).

STRESSES IN THE ZONE OF THE WETTING LINE AND THE DYNAMIC RESISTANCE OF THE MENISCUS

B. V. Zheleznyi and A. G. Nikiforov

UDC 532.68

INTRODUCTION

The use of the usual "condition of adhesion" of a liquid to a solid surface in the analysis of the flow in the zone of the line of solid/liquid/gas three-phase contact (LTC) leads to a solution with mathematical singularities at the line of three-phase contact [1]. Remaining within the framework of the continuum mechanics of a liquid, these singularities can be eliminated either by renouncing the condition of adhesion for the zone of the line of three-phase contact or by assuming that the solid surface near the meniscus is covered with a polymolecular (liquid) film, so that the line of three-phase contact, as such, is absent (there is no "wetting line," but only a finite extension of the transitional region between the meniscus and a film of homogeneous thickness). In the latter case, the condition of adhesion can be used.

The problem of the motion of the meniscus with the presence of a liquid film on the wall is formulated in [2, 3]. The difference between the "departing" and "arriving" menisci is connected with the fact that, in the first case, the mean thickness h_* of the film (remaining on the wall) is determined by the velocity of the meniscus v, while, in the second case, the thickness h_* of the film ahead of the meniscus can be given arbitrarily. In the case of the presence of an additional independent variable (h_*), the case of an arriving meniscus is mathematically more complicated.

The principal practical problem, solvable for a departing meniscus, is to find the dependence $h_*(v)$, while, for an arriving meniscus, it is to find the effective hydrodynamic resistance. The first problem was solved in [2], taking account of the specific thermodynamic and rheological properties of "thin" films, while the second problem was solved in [3] for the case of rather "thick" films having the properties of a volumetric liquid. In the latter

Leningrad. Translated from Zhurnal Prikladnoi Mekhaniki i Tekhnicheskoi Fiziki, No. 4, pp. 116-123, July-August, 1978. Original article submitted June 9, 1977.

0021-8944/78/1904-0515$07.50